Cell

WHAMM Is an Arp2/3 Complex Activator That Binds Microtubules and Functions in ER to Golgi Transport

Kenneth G. Campellone,[1,*] Neil J. Webb,[1] Elizabeth A. Znameroski,[1] and Matthew D. Welch[1,*]
[1]Department of Molecular and Cell Biology, University of California, Berkeley, CA 94720, USA
*Correspondence: campellone@berkeley.edu (K.G.C.), welch@berkeley.edu (M.D.W.)
DOI 10.1016/j.cell.2008.05.032

SUMMARY

The Arp2/3 complex is an actin nucleator that plays a critical role in many cellular processes. Its activities are regulated by nucleation-promoting factors (NPFs) that function primarily during plasma membrane dynamics. Here we identify a mammalian NPF called WHAMM (*WASP homolog associated with actin, membranes, and microtubules*) that localizes to the *cis*-Golgi apparatus and tubulo-vesicular membrane transport intermediates. The modular organization of WHAMM includes an N-terminal domain that mediates Golgi membrane association, a coiled-coil region that binds microtubules, and a WCA segment that stimulates Arp2/3-mediated actin polymerization. Overexpression and depletion studies indicate that WHAMM is important for maintaining Golgi structure and facilitating anterograde membrane transport. The ability of WHAMM to interact with microtubules plays a role in membrane tubulation, while its capacity to induce actin assembly promotes tubule elongation. Thus, WHAMM is an important regulator of membrane dynamics functioning at the interface of the microtubule and actin cytoskeletons.

INTRODUCTION

The actin cytoskeleton is a critical regulator of cell migration, internalization of extracellular material, and vesicle movement (Kaksonen et al., 2006; Pollard and Borisy, 2003). Actin nucleation, the initiation of new filament formation from monomers, is a pivotal step in the regulation of actin assembly (Carlier and Pantaloni, 2007). One factor that both nucleates actin and organizes branched filament networks is the Arp2/3 complex, an evolutionarily conserved protein complex composed of the *a*ctin *r*elated *p*roteins Arp2 and Arp3, which likely act as a template for nucleation, and the additional subunits ARPC1-5, which contribute to nucleation and filament binding (Goley and Welch, 2006).

For Arp2/3 to efficiently nucleate filaments, it must be engaged by *n*ucleation-*p*romoting *f*actors (NPFs) (Millard et al., 2004; Stradal and Scita, 2006). Most mammalian NPFs are members of the (class I) *W*iskott-*A*ldrich *s*yndrome *p*rotein (WASP) family. WASP is found only in hematopoetic cells, but its closest homolog, N-WASP, and the more distant relatives, Scar/WAVE1-3, are expressed more broadly. The nucleation-promoting functions of all family members reside in their C-terminal WCA domains, comprised of *W*ASP *h*omology *2* (WH2) peptides that bind actin monomers, plus *c*onnector and *a*cidic (CA) segments that interact with the Arp2/3 complex. In addition to the WASP family, a second type of NPF (class II), exemplified by cortactin, contains an Arp2/3-interacting acidic region but binds actin filaments instead of monomers (Cosen-Binker and Kapus, 2006; Daly, 2004).

Although the WASPs and WAVEs stimulate Arp2/3 by a conserved mechanism, their activities are differentially modulated by their N-terminal sequences. In the absence of other factors, the nucleation-promoting abilities of the WASPs are low because their WCA regions are masked by intramolecular autoinhibitory interactions with a central *G*TPase-*b*inding *d*omain (GBD) (Kim et al., 2000; Prehoda et al., 2000). Unlike the WASPs, the WAVEs are not autoinhibited. Instead, their NPF activities are suppressed by intermolecular interactions between an N-terminal *S*car-*h*omology *d*omain (SHD) and a complex of regulators (Eden et al., 2002; Innocenti et al., 2004; Steffen et al., 2004).

In addition to these differences, the WASPs and WAVEs are also recruited and activated by distinct signaling molecules, including phosphoinositides, Rho family GTPases, and proteins containing *S*rc-*h*omology-*3* (SH3) domains (Millard et al., 2004; Stradal and Scita, 2006). As a consequence, the WASPs and WAVEs regulate many Arp2/3-related processes at the plasma membrane. For example, cells genetically lacking N-WASP or silenced for N-WASP expression by RNA interference (RNAi) have deficiencies in endocytosis and membrane ruffling (Benesch et al., 2005; Innocenti et al., 2005; Legg et al., 2007). Similarly, WAVE1 and WAVE2 are important for membrane ruffling, lamellipodia formation, and cell migration (Innocenti et al., 2005; Suetsugu et al., 2003; Yamazaki et al., 2003; Yan et al., 2003). Cortactin also plays a regulatory role in many of these processes (Cosen-Binker and Kapus, 2006; Daly, 2004).

Compared to their roles at the plasma membrane, functions for NPFs and Arp2/3 at the surface of internal organelles are not well characterized. Nevertheless, N-WASP is critical for the actin-mediated rocketing of intracellular vesicles rich in $PI(4,5)P_2$ (Benesch et al., 2002). N-WASP can also localize

to the Golgi apparatus and may affect retrograde transport (Egea et al., 2006; Hehnly and Stamnes, 2007). WAVE2 does not localize to the Golgi but promotes Golgi polarization in the direction of cell migration (Magdalena et al., 2003). Lastly, cortactin can regulate vesicle budding at the *trans*-Golgi network (Cao et al., 2005).

Since the identification of the WASPs and WAVEs as Arp2/3 activators nearly a decade ago, much progress has been made in understanding how they regulate nucleation. However, to understand the breadth of Arp2/3 functions, it is necessary to characterize the entire repertoire of proteins that regulate this complex. In the current study, we identify a new NPF called WHAMM, for *W*ASP *h*omolog associated with *a*ctin, *m*embranes, and *m*icrotubules, which activates the Arp2/3 complex in vitro and in cells. Unlike other NPFs, WHAMM regulates ER to Golgi transport and interacts with both the actin and microtubule cytoskeletons to control membrane tubulation and dynamics.

RESULTS

WHAMM Is an Actin Nucleation-Promoting Factor

To identify new activators of the Arp2/3 complex, we surveyed the human proteome for sequences similar to those in the WCA domain of WASP. This search uncovered a predicted protein of 809 amino acids denoted as KIAA1971/WHDC1 (*W*H2 *d*omain *c*ontaining *1*), which we have renamed WHAMM as detailed below (Figure 1A). *WHAMM* is found in the genomes of vertebrates but not in those of *D. melanogaster* or *C. elegans* (Figure S1 available online). Its C-terminal WCA domain includes two putative WH2 peptides and a conserved tryptophan (W807) implicated in Arp2/3 complex activation (Marchand et al., 2001). WHAMM also contains a polyproline region that is predicted to bind profilin. Specific to WHAMM are an N-terminal domain with no significant homology to known proteins and a central portion predicted to form coiled-coils. Overall, WHAMM is <20% similar to other class I NPFs but is roughly 35% identical and 50% similar to JMY (Figure S1), a nuclear factor that controls p53-mediated apoptosis (Shikama et al., 1999).

To evaluate the biochemical function of WHAMM, we first purified N-terminally His-tagged WHAMM (His-WHAMM) from insect cells infected with a recombinant baculovirus (Figure 1B). We also purified a recombinant WCA segment (His-WCA) and raised antibodies against this domain. Immunoblotting with these antibodies revealed that purified His-WHAMM comigrated with native WHAMM from porcine brain extracts as a protein slightly larger than 100 kDa (Figure 1B), indicating that WHAMM is actually expressed in mammalian tissue.

Because WHAMM contains a WCA domain, we next tested its capacity to promote actin nucleation in pyrene-actin polymerization assays (Pollard, 2007). As expected, neither WHAMM nor Arp2/3 efficiently nucleated actin assembly by itself. However, in the presence of Arp2/3, increasing concentrations of His-WHAMM caused a dose-dependent acceleration of actin assembly (Figure 1C), demonstrating that WHAMM is an NPF. The isolated His-WCA domain of WHAMM also stimulated nucleation with Arp2/3. His-WHAMM was slightly more active than His-WCA (Figures 1C and 1E); therefore the recombinant full-length protein is not tightly autoinhibited. In addition, mutation of the conserved tryptophan 807 to alanine in either full-length WHAMM or in the minimal WCA derivative caused a defect in NPF activity relative to the wild-type (WT) proteins, as measured by increases in the times to half maximal actin polymerization and decreases in filament elongation rates at multiple WHAMM concentrations (Figures 1D and 1E). Thus, as with other NPFs, the WCA domain of WHAMM is crucial for full NPF function in vitro.

To compare the activity of WHAMM with other class I NPFs, we expressed and purified His-tagged versions of the WCA domains of WHAMM, N-WASP, and WAVE2 from *E. coli* (Figure S2) and again measured the times to half maximal polymerization and elongation rates (Figure 1F). WHAMM activity was comparable to that of WAVE2 at low concentrations (50–100 nM) but was 2- to 4-fold lower than WAVE2 at higher concentrations. Both WHAMM and WAVE2 were less active than N-WASP. As expected, mutation of the conserved tryptophan residue in the acidic domain of each NPF resulted in a decrease in Arp2/3 complex activation, although WAVE2 was more sensitive to this substitution than WHAMM or N-WASP (Figure S2). Overall, WHAMM shares characteristics with both the WAVE and WASP proteins. It is constitutively active and possesses NPF activity comparable to WAVE2 but has two WH2 domains and exhibits only partial sensitivity to a tryptophan mutation like N-WASP.

WHAMM Associates with Golgi and ERGIC Membranes and Microtubules

To investigate the cellular function of WHAMM, we first sought to examine its expression levels in various human and mouse tissues by immunoblotting. We found that WHAMM was expressed in most organs and was found at particularly high levels in brain tissue (Figures 2A and S1). WHAMM was also expressed in all cultured cell lines that we tested, including monkey (Cos7), human (356HFF), and mouse (NIH 3T3) fibroblasts and human (HeLa) epithelial cells (Figure 2B), suggesting that it is expressed ubiquitously.

Since other NPFs function adjacent to cellular membranes, the ability of WHAMM to associate with membranes was assessed by fractionating cell lysates into membrane and cytosolic components. Immunoblotting demonstrated that WHAMM was found in both fractions but was highly enriched in the membrane sample (Figure 2C). This behavior was more similar to the class I NPF N-WASP than to the class II NPF cortactin. The control proteins transferrin receptor and α-tubulin were found exclusively in the membrane and cytosolic fractions, respectively, confirming the fidelity of the fractionation procedure. WHAMM is only peripherally associated with membranes because treatment with buffers containing a high salt concentration or alkaline pH released it into the soluble fraction (Figure S3).

To ascertain whether WHAMM localizes to the plasma membrane or internal membranes, fixed cells were examined by fluorescence microscopy using antibodies raised against the WHAMM coiled-coil region. Interestingly, unlike other NPFs, WHAMM localized primarily to a perinuclear compartment near the *m*icro*t*ubule-*o*rganizing *c*enter (MTOC) (Figure 2D). In some cells, it was also detected on tubulo-vesicular structures in the cell periphery that frequently localized along microtubules

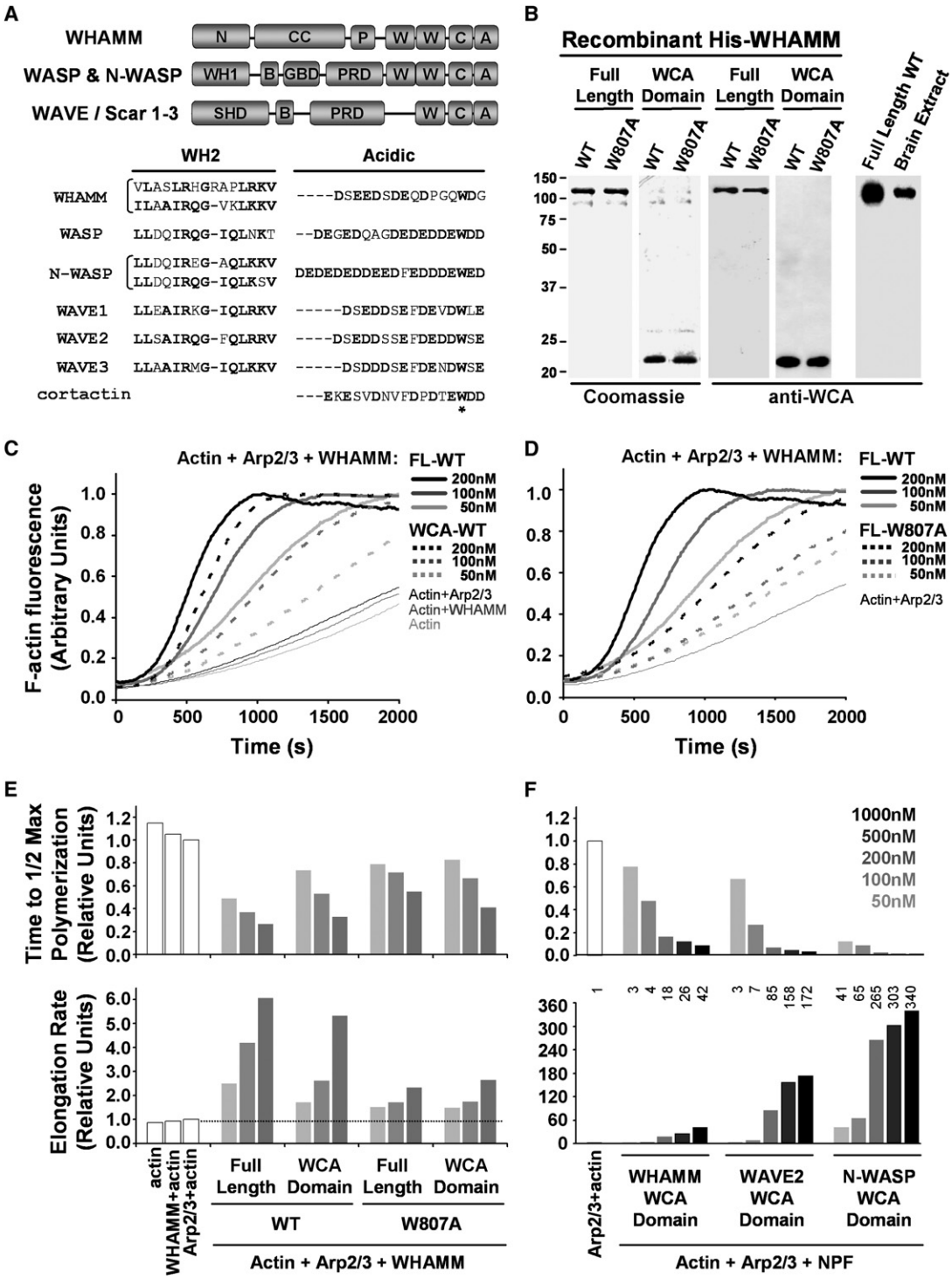

Figure 1. WHAMM Is an Actin Nucleation-Promoting Factor In Vitro

(A) Domain organizations and sequence alignments of WHAMM and other NPFs are shown. Conserved and acidic residues are highlighted in bold.

(B) Purified full-length His-WHAMM and His-WCA were separated by SDS-PAGE and stained with Coomassie blue or blotted with anti-WHAMM WCA antibodies.

(C and D) Actin (2 μM) was polymerized in the presence of 200 nM full-length (FL) His-WHAMM or 20 nM Arp2/3 complex ± His-WHAMM derivatives.

(E and F) Relative times to half-maximal F-actin concentration and elongation rates at these times are shown in the presence of Arp2/3 and various His-NPFs.

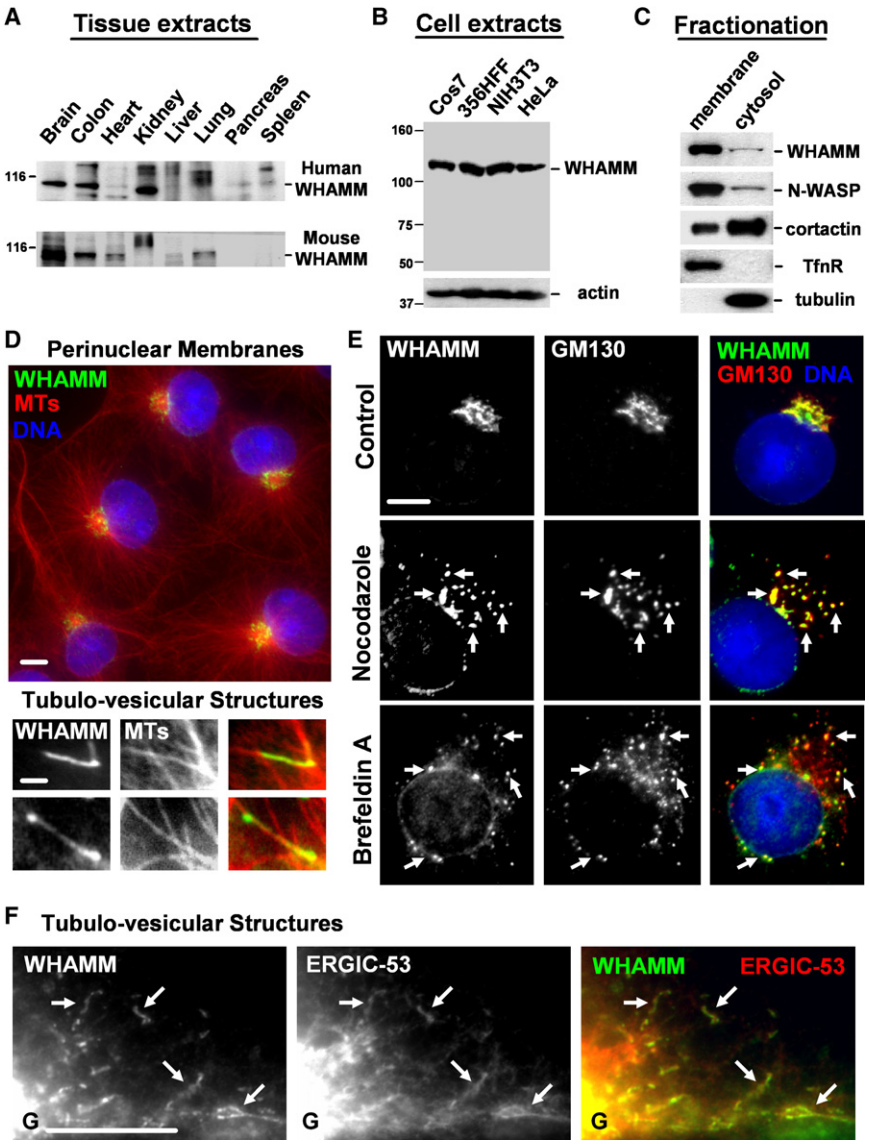

Figure 2. WHAMM Associates with Golgi and ERGIC Membranes and Microtubules

(A and B) Extracts from human and mouse organs (15 μg/lane) or from Cos7, human foreskin fibroblast, NIH 3T3, and HeLa cells were blotted with anti-WHAMM WCA antibodies. Anti-actin blotting was used to normalize protein content.

(C) Membrane and cytosolic fractions from Cos7 cells were blotted for the indicated proteins.

(D) Cos7 cells were stained with antibodies to the WHAMM CC domain, α-tubulin (MTs), and DAPI. Scale bars: top, 10 μm; bottom, 1 μm.

(E) Cells were treated with a media control, nocodazole, or brefeldin A and stained with antibodies to WHAMM, GM130, and DAPI. Arrows highlight colocalization. Scale bar: 10 μm.

(F) Cells expressing GFP-ERGIC-53 were stained for WHAMM and GFP (pseudocolored red). Golgi positioning is indicated (G) and arrows highlight tubule colocalization. Scale bar: 10 μm.

(Figure 2D). Thus, we propose that a more descriptive name for KIAA1971/WHDC1 is WHAMM.

Because the Golgi apparatus is known to be clustered near the MTOC, we sought to determine if WHAMM colocalized with markers for different subcompartments of the Golgi. In fact, WHAMM colocalized extensively with the *cis*-Golgi protein GM130 (Figure 2E) but did not precisely overlap with the medial and *trans*-Golgi markers GalT and TGN46 (Figure S4). WHAMM localization did not coincide with stains for other organelles such as the endoplasmic reticulum (ER), recycling endosomes, or mitochondria (Figure S4). We confirmed that WHAMM associates mainly with the *cis*-Golgi by treating cells with nocodazole to depolymerize microtubules or brefeldin A to inhibit Arf GTPases, two conditions that disperse the *cis*-Golgi from the MTOC. In each case, WHAMM was redistributed into cytoplasmic puncta in patterns that maintained frequent colocalization with GM130 (Figure 2E).

The observation that WHAMM also localizes along tubulo-vesicular structures raised the possibility that it associates with membrane transport intermediates that move between the ER and Golgi. One organelle that is situated close to the Golgi and also in peripheral tubules is the *ER-Golgi intermediate compartment* (ERGIC) (Appenzeller-Herzog and Hauri, 2006). To test whether the WHAMM-associated tubules comprise part of this organelle, cells were transfected with GFP-ERGIC-53, a transmembrane ERGIC marker, and stained for WHAMM. In cells expressing low levels of GFP-ERGIC-53, this protein sometimes overlapped with *cis*-Golgi-associated WHAMM near the MTOC (Figures S5 and S6). WHAMM and GFP-ERGIC-53 also colocalized along peripheral tubules (Figure 2F), suggesting that many WHAMM-associated tubulo-vesicular membranes represent ER-Golgi intermediates.

Distinct WHAMM Domains Mediate Interactions with Membranes and Microtubules

To investigate how its localization is determined, WHAMM was fused to fluorescent protein tags including GFP, mCherry, and LAP (*l*ocalization and *a*ffinity *p*urification; comprised of a His-GFP-S tag) (Table S1) and expressed in cultured cells. Fractionation and immunoblotting revealed that LAP-WHAMM, like endogenous WHAMM, was enriched on membranes, although the levels of cytosolic WHAMM became elevated when it was highly overexpressed (Figure 3A). Consistent with these results, when cells harbored low amounts of LAP-WHAMM, it was visible in the Golgi region (Figure 3B). Expression of LAP-WHAMM at intermediate levels resulted in fluorescence at the Golgi and tubular membranes lying along microtubules (see inset), although

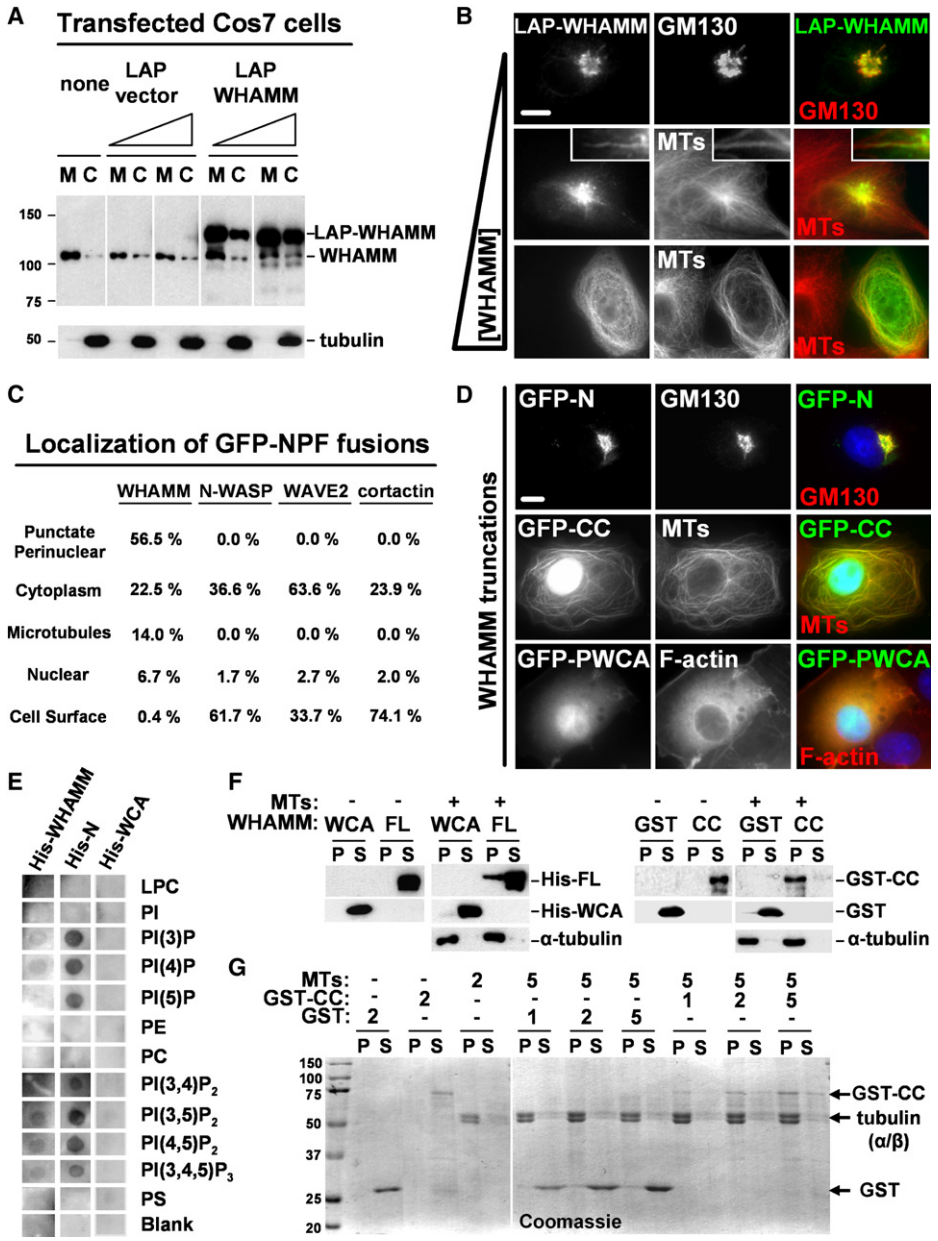

Figure 3. Distinct WHAMM Domains Mediate Interactions with Membranes and Microtubules

(A) Cos7 cells transfected with 35 or 150 ng of LAP or LAP-WHAMM plasmids were fractionated into membranes (M) and cytosol (C) and blotted for WHAMM and α-tubulin.

(B) Cells transfected with 35, 100, or 250 ng of LAP-WHAMM plasmid were stained for GM130 or α-tubulin (MTs). Scale bar: 10 μm. Insets show a 10 μm long tubulo-vesicular structure.

(C) Cells transfected with 100 ng of NPF plasmids were stained with phalloidin and anti-α-tubulin. GFP localizations were assessed visually. The total % of cells with a given localization was determined by scoring >200 cells for each NPF in three experiments.

(D) Cells expressing intermediate levels of GFP-WHAMM truncations were stained with antibodies to GM130 or α-tubulin or with phalloidin (F-actin). Scale bar: 10 μm.

(E) Membrane strips containing 100 pmol spots of phospholipids were overlayed with His-WHAMM derivatives. Bound WHAMM was detected by anti-His blotting.

(F and G) His-WHAMM, His-WCA, GST, or GST-CC (200 nM in F; 1–5 μM in G) were centrifuged ± microtubules (1 μM in F; 2–5 μM in G). Proteins in pellet (P) or supernatant (S) fractions were visualized by blotting with anti-WHAMM WCA, GST, or α-tubulin antibodies (F) or with Coomassie blue (G).

some cells exhibited cytoplasmic WHAMM localization. Compared to nontransfected cells, more unusually long (>10 μm) tubules were found in cells with intermediate levels of LAP-WHAMM, suggesting that its expression increases tubulation. Lastly, cells with very high amounts of LAP-WHAMM displayed a reorganization of microtubules from a radial array originating at the MTOC to peripheral bundles coated with LAP-WHAMM (Figure 3B).

We next compared GFP-WHAMM localization to that of other GFP-tagged NPFs by quantifying the percentage of transfected cells with punctate perinuclear, cytoplasmic, nuclear, microtubule, or plasma membrane GFP fluorescence. Notably, only GFP-WHAMM exhibited Golgi-like, tubulo-vesicular, or microtubule localizations (Figure 3C). Peripheral GFP-WHAMM tubules did not associate with the plasma membrane because they did not contain the lipid dye DiI (Figure S7). In contrast, the most frequent noncytosolic location of GFP-N-WASP, WAVE2, and cortactin was at the cell cortex (Figures 3C and S8). Thus, WHAMM seems to be more specifically associated with Golgi and ERGIC membranes than other NPFs.

To define the molecular basis for WHAMM recruitment to membranes and microtubules, GFP-WHAMM truncations comprising the N-terminal (GFP-N), coiled-coil (GFP-CC), or C-terminal (GFP-PWCA) domains were expressed and visualized in cells (Figures 3D and S9). GFP-N was found at the *cis*-Golgi, as determined by colocalization with GM130. In contrast, GFP-CC localized along microtubules and in the nucleus. Sustained expression of this fusion resulted in an abnormal bundling of microtubules (Figure S10). Lastly, GFP-PWCA localized diffusely throughout transfected cells and triggered an accumulation of F-actin in the cytoplasm of these cells relative to their nontransfected counterparts, as visualized by phalloidin staining (Figure 3D). Neither the N, CC, nor PWCA fragments were found at elongated tubulo-vesicular membranes, suggesting that these domains need to be present within the same molecule to localize to or generate such structures.

Since the WHAMM N-terminus and coiled-coil region mediate localization to Golgi membranes and microtubules in cells, the abilities of recombinant His-WHAMM or its truncation variants to bind to purified phospholipids or microtubules were assessed in vitro. First, we tested whether His-WHAMM or its N-terminal region (His-N; Figure S9) could bind to synthetic phospholipids immobilized on filter strips in overlay assays. Anti-His immunoblotting indicated that both His-WHAMM and His-N bound to phosphorylated phosphatidylinositols (PIPs), but that His-N exhibited more robust binding (Figure 3E). Neither protein bound to other phospholipids. The His-WCA domain did not bind to any phospholipids, indicating that the observed associations were not due to the His-tag. These results are consistent with the possibility that the WHAMM N terminus directly mediates interactions with membranes.

Next, we examined whether full-length His-WHAMM or its GST-tagged coiled-coil domain (GST-CC; Figure S9) could bind directly to purified microtubules in cosedimentation assays. Immunoblotting indicated that a fraction of His-WHAMM and the majority of GST-CC cosedimented with microtubules, whereas the control proteins His-WCA and GST did not (Figure 3F). Similar assays using GST-CC and microtubules at various molar ratios demonstrated that GST-CC bound microtubules at all concentrations (Figure 3G). None of these proteins were pelleted when centrifuged in the absence of microtubules. Collectively these results indicate that WHAMM possesses a modular domain organization featuring an N terminus that associates with membranes, a coiled-coil region that binds microtubules, and a PWCA domain that promotes actin nucleation.

WHAMM-Mediated Actin Assembly in Cells Requires WCA-Arp2/3 Interactions

The NPF activity of WHAMM in vitro and its localization in cells together suggest that WHAMM can stimulate the Arp2/3 complex at the Golgi and along tubular membranes. Consistent with this hypothesis, Arp3 coprecipitated with LAP-WHAMM, but not the LAP-tag by itself, from transfected cell lysates (Figure 4A). To test whether WHAMM activates Arp2/3 at the Golgi or along tubules, cells expressing GFP-WHAMM were stained for F-actin and Arp3. GFP-WHAMM caused a dramatic increase in F-actin at the Golgi relative to endogenous levels and allowed F-actin and Arp3 to be visualized along tubular structures (Figure 4B). Quantification of F-actin content by visual observations (Figure 4C) and by measurement of fluorescence pixel intensities (Figure S11) revealed significant increases in F-actin staining in cells expressing intermediate to high levels of GFP-WHAMM. Similar increases were detected in cells expressing GFP-WAVE2, but not GFP-N-WASP (Figure 4C), consistent with the idea that WHAMM is not autoinhibited in cells. The WCA region is essential for WHAMM-mediated actin polymerization because a GFP-WHAMMΔWCA mutant did not induce any measurable increase in F-actin content (Figure S11).

To further probe the cellular role of WHAMM WCA-Arp2/3 interactions, WT LAP-WHAMM and a W809A mutant were expressed in control cells and in cells in which the Arp2/3 complex was depleted by RNAi (Figure 4D). Immunoblotting revealed that treatment with siRNAs to Arp3 and ARPC4 resulted in degradation of multiple subunits, while a nonspecific siRNA did not affect their expression (Figure 4E). LAP-WHAMM and the W807A variant were each enriched at the Golgi region in control and Arp2/3-depleted cells, although the mutant formed large vesicles more frequently than WT did (Figures 4D and S11). Visual observations revealed that WT LAP-WHAMM increased the F-actin content in nearly 90% of control cells, while the mutant did so in less than 20% of cells (Figures 4D and 4F), consistent with the reduced ability of the mutant to coprecipitate with Arp3 (Figure 4A). Neither protein triggered actin assembly in Arp2/3-depleted cells (Figures 4D and 4F). These observations indicate that the interactions between the WHAMM WCA domain and the Arp2/3 complex are critical for WHAMM-mediated actin polymerization in cells.

WHAMM Overexpression or Depletion Disrupts the Structure of the Golgi Apparatus

The observation that WHAMM localizes to the ERGIC and Golgi apparatus suggests that it may influence the structure of these organelles. To test this possibility, the effects of altering WHAMM protein levels on the positioning of GFP-ERGIC-53 and the Golgi proteins GM130 and TGN46 were examined. Whereas expression of tagged WHAMM at low levels did not affect ERGIC or Golgi morphology (data not shown), cytoplasmic WHAMM overexpression caused a redistribution of the ERGIC, *cis*-, and *trans*-Golgi networks throughout the cell (Figure 5A). This effect was specific to WHAMM overexpression and not a generic result of Arp2/3 misregulation, as overexpressing other NPFs did not affect Golgi distribution (Figures 5B and S12). Arp2/3 activation was not essential for Golgi disruption because the WHAMM W809A mutant also dispersed the Golgi

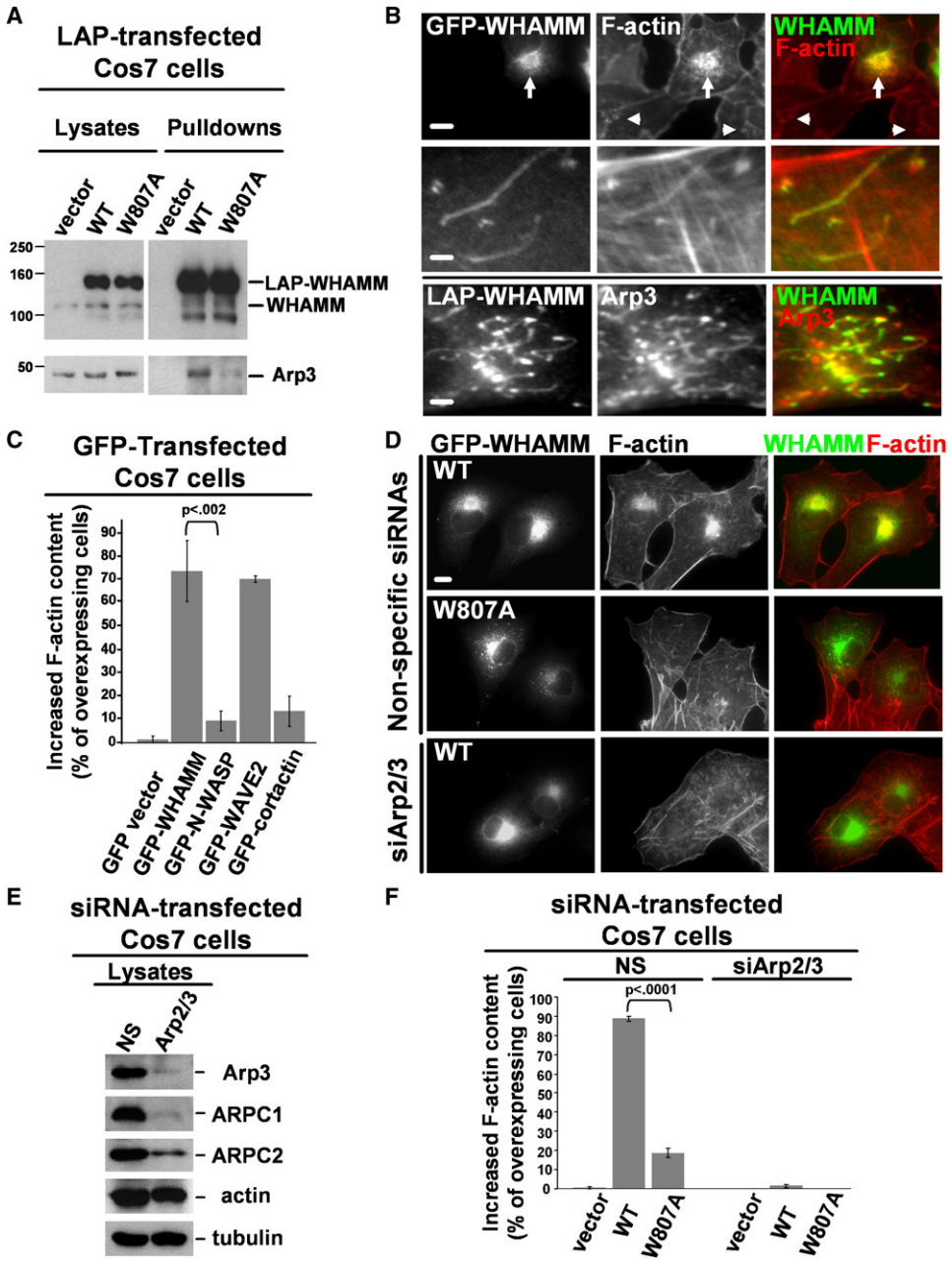

Figure 4. WHAMM-Mediated Actin Assembly in Cells Requires WCA-Arp2/3 Interactions

(A) Cos7 cells expressing LAP-tagged variants were subjected to SDS-PAGE directly (lysates) or treated with magnetic beads to collect tagged proteins prior to SDS-PAGE (pulldowns). Proteins were visualized by blotting with antibodies to WHAMM WCA and Arp3.

(B) Cells expressing tagged WHAMM were stained with phalloidin (F-actin) or Arp3 antibodies. Arrows show increased F-actin content at the Golgi; arrowheads, endogenous Golgi F-actin. Scale bars: top, 10 μm; middle and bottom, 1 μm.

(C) Cells transfected with GFP-NPFs and exhibiting intermediate to high levels of GFP fluorescence were chosen randomly for examination. The phalloidin fluorescence intensity in transfected (GFP-expressing) cells was visually compared to that in nearby nontransfected cells, and the % of transfected cells with a clear increase in F-actin staining was quantified. Data are the mean ± SEM of two experiments with 50 cells examined per sample.

(D) Cells transfected with siRNAs and LAP-WHAMM plasmids were stained with phalloidin. Scale bar: 10 μm.

(E) Cells treated with a nonspecific (NS) control siRNA or Arp3 and ARPC4 siRNAs were blotted with antibodies to Arp3, ARPC1, and ARPC2, plus actin and α-tubulin as loading controls.

(F) Cells cotransfected with siRNAs and LAP plasmids were visualized as in (C), and the % with increased F-actin content was quantified. Data are the mean ± SEM of four experiments with approximately 50 cells examined per sample.

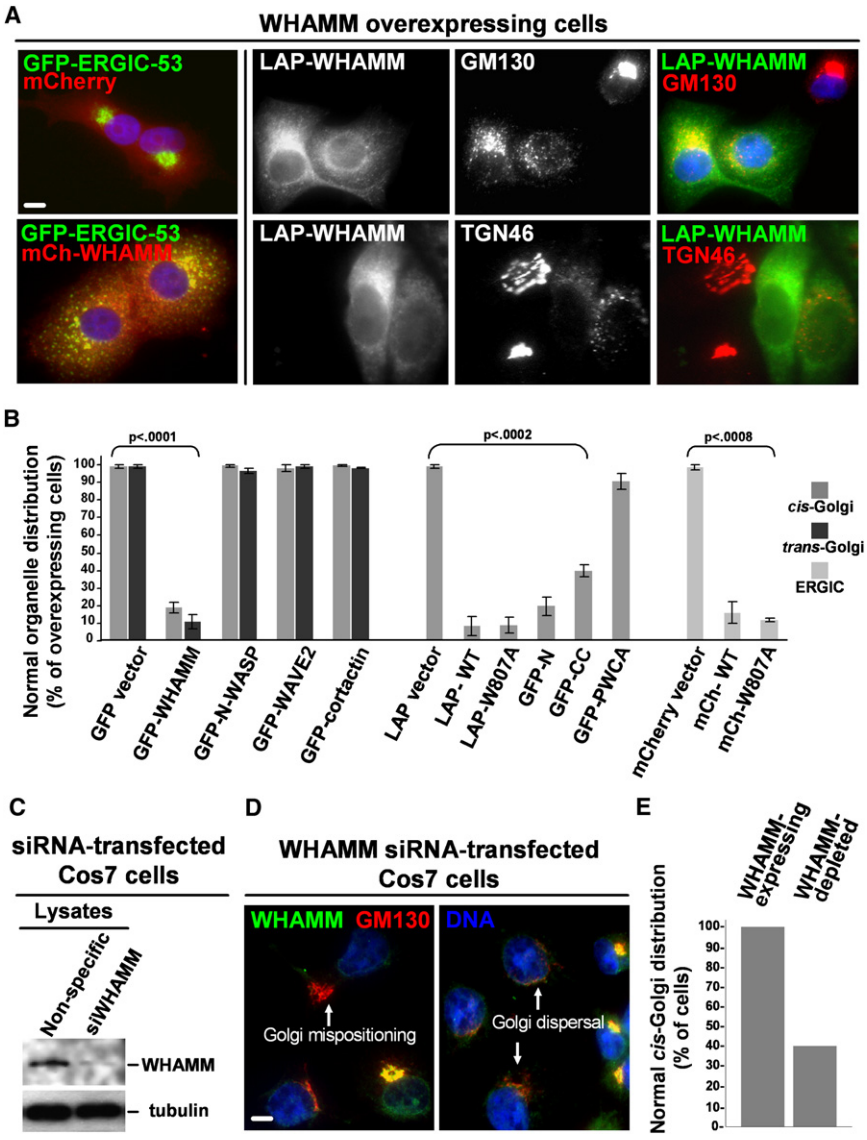

Figure 5. WHAMM Overexpression or Depletion Disrupts Golgi Structure

(A) Cos7 cells expressing GFP-ERGIC-53 were transfected with mCherry or mCherry-WHAMM plasmids (left panels). Cos7 (top) and HeLa (bottom) cells overexpressing LAP-WHAMM were stained with antibodies to GM130 or TGN46. Scale bar: 10 μm.

(B) The % of cells with a normal distribution of GFP-ERGIC-53, GM130 (*cis*-Golgi), or TGN46 (*trans*-Golgi) was quantified in Cos7 cells expressing high levels of NPFs. Data are the mean ± SEM of 2–3 experiments with roughly 50 cells examined per sample.

(C) Cells treated with a nonspecific or WHAMM siRNA were blotted for WHAMM and tubulin.

(D) WHAMM siRNA-treated Cos7 cells were stained for WHAMM and GM130.

(E) The % of WHAMM-depleted or nearby nondepleted Cos7 cells with normal GM130 staining was quantified visually in a representative experiment in which >30 cells were examined per sample. Similar patterns were observed in HeLa cells (not shown). Scale bar: 10 μm.

(Figure 5B), and each protein elicited the same phenotype in Arp2/3-depleted cells (data not shown). To test if the membrane and microtubule interacting sequences of WHAMM are the major contributors to Golgi disruption, GM130 localization was examined in cells overexpressing the GFP-N, GFP-CC, or GFP-PWCA truncations. Among these fragments, GFP-N disrupted Golgi organization most frequently (Figures 5B and S12). The microtubule-binding GFP-CC derivative also caused Golgi dispersal but 2- to 3-fold less frequently than GFP-N. In contrast, GFP-PWCA had little effect on Golgi structure. Thus, the N-terminal and coiled-coil regions of WHAMM are the primary mediators of Golgi reorganization in WHAMM overexpressing cells.

To determine if WHAMM depletion also affects Golgi positioning and morphology, Cos7 and HeLa cells were treated with an siRNA to human WHAMM or with control nonspecific or GAPDH siRNAs. Although cultures receiving the WHAMM siRNA contained fewer adherent cells after 48–96 hr, WHAMM silencing in these cells could be detected by immunoblotting (Figure 5C). Therefore, we determined the effect of WHAMM depletion on Golgi structure by examining individual cells stained with antibodies to WHAMM and GM130. In >99% of cells treated with control siRNAs, WHAMM was readily detectable and GM130 positioning was normal (Figure 5E). In contrast, cells treated with the WHAMM siRNA showed variable WHAMM staining. In the population of cells with no detectable WHAMM, more than 60% had aberrant Golgi features, including mispositioning of GM130 away from the MTOC or redistribution of GM130 into dispersed puncta (Figures 5D and 5E). The Golgi was not lost from these cells because the total GM130 fluorescence content was equivalent in WHAMM-expressing and WHAMM-depleted cells (Figure S12). Thus, WHAMM is an important regulator of Golgi positioning and morphology.

WHAMM Overexpression or Depletion Inhibits Anterograde Transport of VSV-G

To investigate the possibility that WHAMM functions in membrane trafficking, transport of GFP- or mCherry-tagged versions of the temperature-sensitive viral protein VSV-G was examined. When transfected cells are grown at 40°C, VSV-G misfolds and is retained in the ER. Upon a shift to 33°C, it folds and becomes detectable at the Golgi apparatus after 15 min and the plasma membrane by 60 min (Hirschberg et al., 1998; Presley et al., 1997; Scales et al., 1997) (Figure S13). Importantly, after 15 min, many Golgi and tubular VSV-G structures colocalized with WHAMM, implicating WHAMM in VSV-G progression from the ER to the Golgi (Figures 6A and S14).

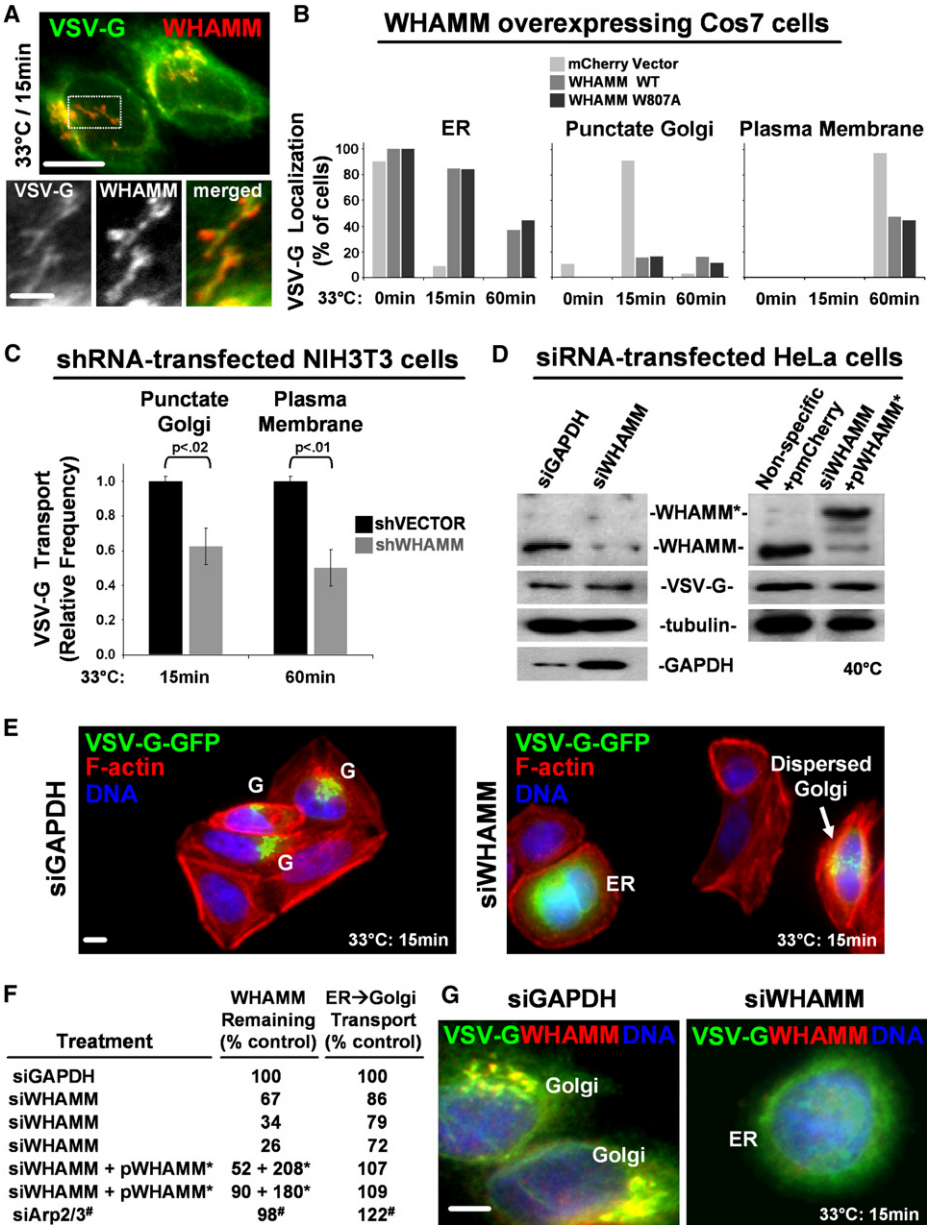

Treatment	WHAMM Remaining (% control)	ER→Golgi Transport (% control)
siGAPDH	100	100
siWHAMM	67	86
siWHAMM	34	79
siWHAMM	26	72
siWHAMM + pWHAMM*	52 + 208*	107
siWHAMM + pWHAMM*	90 + 180*	109
siArp2/3#	98#	122#

Figure 6. WHAMM Overexpression or Depletion Inhibits Anterograde Transport of VSV-G

(A) Cells expressing VSV-G-GFP and shifted to 33°C for 15 min were stained with WHAMM and GFP antibodies. Scale bars: top, 10 μm; bottom, 5 μm.

(B) Cells coexpressing VSV-G-GFP and mCherry-WHAMM were shifted to 33°C for 15 or 60 min. The % with visually apparent ER, Golgi, or plasma membrane GFP fluorescence is shown for a representative experiment in which >25 cells were examined per sample.

(C) The % of shRNA-transfected cells (identified by their GFP fluorescence) with visually apparent Golgi or surface localization of VSV-G-mCherry was quantified and normalized to nearby non-shRNA-transfected control cells. Data are the mean ± SEM from 2–3 experiments in which >35 cells were examined per sample.

(D) Cells treated with siRNAs ± vectors encoding mCherry or siRNA-resistant mCherry-WHAMM* were transfected with VSV-G-GFP and blotted for WHAMM, GFP, tubulin, and GAPDH.

(E) Cells transfected with siRNAs were stained with phalloidin (F-actin). VSV-G-GFP localization to the Golgi (G) or ER is indicated. Scale bar: 10 μm.

(F) WHAMM protein levels were determined by immunoblotting and densitometry and normalized to tubulin. The fraction of cells with punctate Golgi-like fluorescence was measured relative to parallel siGAPDH control samples. Arp2/3 data (#) are the mean of four experiments with approximately 60 cells examined per sample.

(G) Cells transfected with siRNAs were stained for WHAMM and VSV-G-GFP.

To determine the effects of WHAMM overexpression on transport, VSV-G-GFP was cotransfected with mCherry-WHAMM WT or the W807A mutant. Compared to control cells expressing mCherry, cells with high levels of either mCherry-WHAMM protein exhibited a 6-fold decrease in the frequency of punctate Golgi-like VSV-G-GFP fluorescence after 15 min at 33°C

(Figure 6B). This phenotype was not due to Golgi dispersal masking transport because distributed puncta were scored positively for Golgi localization, and in most cells overexpressing WHAMM, VSV-G-GFP fluorescence was observed in a reticular pattern indicative of ER retention (Figures 6B and S15). Consistent with a deficiency in transport, after 60 min the frequency of VSV-G localization at the surface of mCherry-WHAMM-overexpressing cells was less than half that of control cells (Figure 6B). Since both WT WHAMM and the W807A mutant inhibited trafficking of VSV-G, this effect is independent of robust Arp2/3 activation.

To further probe the role of WHAMM during transport, it was depleted by RNAi. First, NIH 3T3 cells harboring plasmids encoding short hairpin (sh)RNAs to murine WHAMM or a vector control (each coexpressing GFP) were transfected with a VSV-G-mCherry plasmid. VSV-G localization was then observed following temperature shifts. Compared to cells treated with the vector control, cells receiving the shWHAMM plasmids (identified by GFP fluorescence) transported VSV-G to the Golgi 40% less frequently after 15 min at 33°C and showed a 50% reduction in plasma membrane localization of VSV-G after 60 min (Figure 6C).

For an independent assessment of transport, VSV-G-GFP progression to the Golgi was examined in HeLa cells depleted of WHAMM using siRNAs (Figure 6D). Compared to siGAPDH-treated cells, fewer siWHAMM-treated cells exhibited Golgi-like VSV-G fluorescence after 15 min at 33°C, and when VSV-G was present in punctate structures, these puncta were more dispersed than the Golgi in control cells (Figure 6E). Importantly, the level of WHAMM silencing correlated with reduced transport (Figure 6F). When WHAMM protein was decreased by almost 75%, as determined by blotting and densitometry, VSV-G transport was reduced by nearly 30% relative to the GAPDH control. Moreover, in cells lacking visible WHAMM, VSV-G was retained in the ER (Figures 6G and S14). This defect was specific to WHAMM depletion because transport in WHAMM siRNA-treated cells was rescued by low-level expression of siRNA-resistant mCherry-WHAMM* (Figures 6D and 6F), and cells lacking N-WASP or WAVE2 transported VSV-G normally (not shown). VSV-G movement did not require the Arp2/3 complex because Arp2/3-depleted cells exhibited a 20% increase in transport (Figure 6F). This result may be due to the fact that Arp2/3-depleted cells possess less perinuclear F-actin (Figure S16), which may affect transport. Overall, overexpression and depletion studies highlight an important role for WHAMM in regulating ER to Golgi transport and suggest that this function does not absolutely require its NPF activity.

WHAMM Tubule Dynamics Require Interactions with Microtubules and Actin Filaments

The observation that WHAMM interacts with membranes, microtubules, and actin implies that it might mediate cytoskeletal crosstalk during membrane movement. To explore this possibility, the behavior of GFP- or mCherry-WHAMM-associated membranes was observed in live cells expressing low to intermediate levels of these proteins. Tagged WHAMM was visible both on spherical vesicles and on tubulo-vesicular structures moving throughout the cell (Figure 7A; Movie S1). Some dynamic tubulo-vesicular membranes are apparently part of the ERGIC because they recruited both mCherry-WHAMM and GFP-ERGIC-53 (Figure 7B). WHAMM-associated tubules exhibited a variety of movements, including elongation, contraction, spiraling, and branching (Figure 7A; Movie S2). The formation of tubules was only visible in cells expressing full-length tagged WHAMM and not the truncated GFP-N, CC, or PWCA proteins, suggesting that multiple domains cooperate during tubule formation.

Since some tubular mCherry-WHAMM membranes were aligned along microtubules labeled with GFP-tubulin (Figure 7B), we reasoned that microtubules might play a role in their dynamics. To test this notion, GFP-WHAMM-expressing cells were treated with taxol to stabilize microtubules or nocodazole to promote their depolymerization. While taxol did not affect membrane dynamics, nocodazole caused GFP-WHAMM vesicles to stop moving (Table S2). Nocodazole also prevented the formation of GFP-WHAMM tubules, stopped the motility of pre-existing tubules, and sometimes promoted the dissolution of tubules into smaller structures (Figure 7C; Movie S3). These results are consistent with a requirement for microtubules and their motors for vesicle movement as well as membrane tubule formation, elongation, and stability.

Importantly, GFP-WHAMM tubulo-vesicular structures also recruited mCherry-actin (Figure 7B) and elongated at a mean rate of 6.7 μm/min (n = 12), a speed consistent with actin-based movement (Pollard and Borisy, 2003). To investigate the role of actin dynamics in vesicle and tubule movements, cells were treated with cytochalasin D, a drug that binds barbed ends and inhibits filament elongation, jasplakinolide, an F-actin stabilizing agent, or latrunculin A, a toxin that sequesters actin monomers and triggers filament disassembly. Although cytochalasin had no effect on vesicle movement, it caused tubules to stop elongating (Figure 7C; Movie S4). Jasplakinolide also halted tubule dynamics (Table S2), demonstrating that actin turnover is important for tubule motility. Lastly, latrunculin caused a collapse of long WHAMM tubules into large vesicles (Figure 7C; Movie S5). Collectively, these results indicate that actin filaments are necessary for the elongation and stabilization of WHAMM-associated tubular membranes.

Finally, to define the role of WHAMM NPF activity in membrane dynamics, the movement of membranes associated with the GFP-WHAMM W807A mutant was examined. Interestingly, these tubulo-vesicular structures appeared to have a defect in elongation. While many WT WHAMM-associated tubules elongated continuously for distances >10 μm, mutant tubules did not extend more than 1–2 μm before shrinking (Figure 7D; Movie S6). Moreover, the mean percentage of time that WT tubules spent elongating was more than three times greater than that of W807A tubules (Figure 7D). Thus, the WHAMM WCA domain seems to enable efficient tubule elongation by triggering Arp2/3-mediated actin assembly. The observation that microtubules and actin filaments both control membrane tubulation highlight a role for WHAMM in coordinating interactions with both cytoskeletal systems during membrane dynamics.

DISCUSSION

For nearly a decade, insights into the function of the Arp2/3 complex have been obtained by characterizing the activities of its

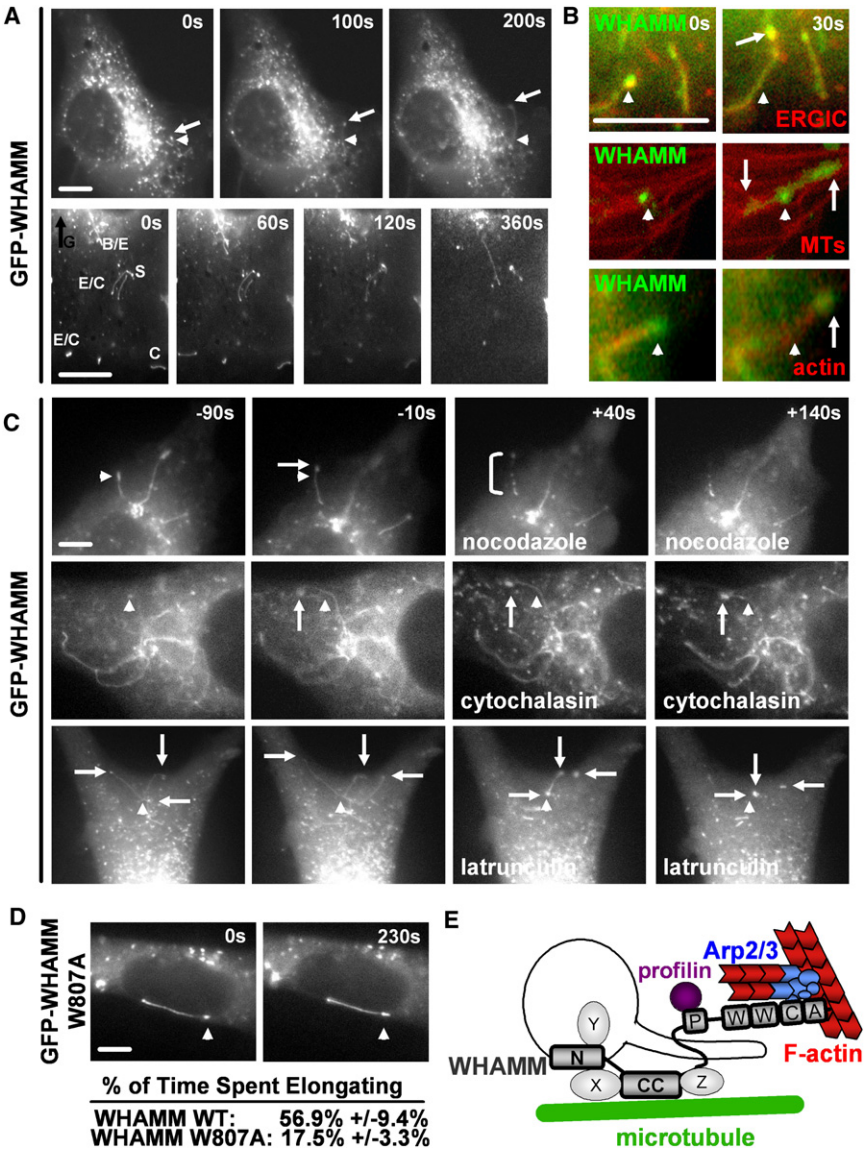

Figure 7. WHAMM Tubule Dynamics Require Interactions with Microtubules and F-Actin

(A) Cos7 cells expressing GFP-WHAMM were visualized by timelapse microscopy. In all panels, arrowheads point to a fixed position and arrows indicate moving ends of dynamic tubules. Enlargements of elongating (E), contracting (C), spiraling (S), and branching (B) structures in the cell periphery away from the dense Golgi (G) are shown. Scale bars: 10 μm.

(B) Cells expressing GFP-ERGIC53, GFP-tubulin, or mCherry-actin (all in red) and mCherry- or GFP-WHAMM (all in green) were observed.

(C) NIH 3T3 cells expressing GFP-WHAMM were visualized before and after treatment with nocodazole, cytochalasin, or latrunculin. The bracket indicates an example of membrane dissolution.

(D) Cells expressing GFP-WHAMM W809A or WT were visualized and the % of time (mean ± SEM) that tubules spent elongating were compared ($n = 35$ each; $p < .0001$).

(E) A model for WHAMM function during membrane tubulation is shown.

regulators, the WASPs and WAVEs. Here, we uncovered WHAMM as a related Arp2/3 activator. However, unlike other NPFs, WHAMM regulates ER to Golgi transport and interacts with both the actin and microtubule cytoskeletons to control membrane tubulation and dynamics. The observation that WHAMM is present specifically in vertebrate cells suggests that different proteins may carry out WHAMM-like activities in other organisms or that the mechanisms of membrane transport differ between species.

Among the characteristics that WHAMM shares with class I NPFs is the manner in which it stimulates nucleation (Millard et al., 2004; Stradal and Scita, 2006). It possesses two apparent WH2 domains as well as a tryptophan residue in its acidic region that is important for triggering Arp2/3-mediated actin assembly in vitro and in cells. However, the regulation of WHAMM NPF activity more closely resembles that of the WAVEs than that of the WASPs because full-length WHAMM is constitutively active in vitro and triggers actin assembly when expressed in cells, implying that it is not tightly autoinhibited and may be regulated by binding partners.

The first evidence that WHAMM participates in a cellular function different from that regulated by the WASPs, WAVEs, or the recently identified WASH protein (Linardopoulou et al., 2007) is the observation that WHAMM localizes to the *cis*-Golgi and ERGIC rather than the plasma membrane or endosomes. Although Arp2/3 has been detected at the Golgi, its ability to trigger actin assembly in response to NPFs at this site is not well understood (Egea et al., 2006; Hehnly and Stamnes, 2007). Our results indicate that WHAMM and Arp2/3 can interact to promote actin assembly both at the Golgi apparatus and along tubular membranes. In addition, WHAMM causes a disruption in the localization and organization of the Golgi apparatus when overexpressed or when silenced. These results suggest that WHAMM is important for controlling the normally compact and stacked Golgi structure and situating it near the MTOC, perhaps due to its ability to associate with both Golgi membranes and microtubules.

By monitoring the localization of the VSV-G protein, some WHAMM-associated tubular membranes were revealed to be transport intermediates directed from the ER to the *cis*-Golgi. When WHAMM was overexpressed, VSV-G transport to the cell surface was reduced, likely as a result of defective ER to Golgi transport. This phenotype could be due to a mislocalization of secretory components or stimulation of retrograde transport in the presence of excess WHAMM. Notably, in complementary WHAMM-depletion experiments, VSV-G progression

from the ER to the Golgi, and ultimately the cell surface, was also diminished. Such sensitivity to WHAMM protein levels suggests that WHAMM is important for anterograde transport in normal cells.

Somewhat surprisingly, the NPF activity of WHAMM is not essential for disrupting VSV-G transport. It seems plausible that, in the absence of WCA-Arp2/3-mediated tubulation events or densely packed F-actin networks near the Golgi, VSV-G is transported more rapidly via small vesicular carriers rather than large tubular structures (Simpson et al., 2006). It is also possible that WCA-Arp2/3-derived actin assembly facilitates transport of secretory cargo that is sorted differently than VSV-G, or that WHAMM NPF activity is important for controlling retrograde pathways. The observation that some WHAMM tubules do not colocalize with VSV-G is consistent with either of these possibilities.

While a defined role for WHAMM during vesicular transport requires further investigation, a model for how WHAMM acts during tubular transport (Figure 7E) has emerged from a combination of in vitro biochemical assays, cellular expression of WHAMM derivatives, and live-cell analyses. These studies indicate that WHAMM has a modular domain structure featuring an N terminus that interacts with membranes and a coiled-coil region that binds microtubules. Together, these domains may cooperate to form a functional unit for deforming or moving membranes. The observation that microtubule depolymerization prevents elongation of WHAMM-associated membranes further suggests that microtubules or their motors may be necessary for tubulation. In fact, microtubules and motors can initiate tubule formation from ER and Golgi membranes in vitro (Upadhyaya and Sheetz, 2004). Importantly, actin nucleated by the WHAMM WCA domain seems to stabilize the tubulated membrane state and facilitate its elongation. Although it seems likely that the long extensions visualized by expression of WT GFP-WHAMM are an exaggeration of the normal structures detected in cells expressing WHAMM at endogenous levels, they also highlight the fact that WCA-mediated actin nucleation is important for increasing membrane tubulation.

Interestingly, crosstalk between proteins that deform membranes and those that control actin assembly has been uncovered during both endocytosis and cell-surface protrusion (Itoh et al., 2005; Mattila et al., 2007; Tsujita et al., 2006). Endocytic regulators with F-BAR or EFC domains bind to the plasma membrane to form tubular invaginations and also recruit N-WASP to stimulate actin assembly and the GTPase dynamin to trigger membrane fission (Itoh et al., 2005; Merrifield et al., 2005; Tsujita et al., 2006; Yarar et al., 2005). However, the relationships between F-actin and membrane tubulation may be different at the cell surface than at membranes moving between the ER and Golgi because invagination is enhanced by depolymerizing actin filaments with latrunculin (Itoh et al., 2005; Tsujita et al., 2006), whereas the same treatment causes a collapse of WHAMM-associated tubules. Thus, F-actin could provide tension along ER or Golgi membranes to facilitate their tubulation or movement.

Given its interactions with actin, membranes, and microtubules, a further understanding of WHAMM activities holds promise for uncovering many intriguing aspects of membrane and cytoskeletal dynamics. Transport between the ER and Golgi apparatus is known to be controlled by a number of small GTPases from the Sar, Rab, and Arf families (Lee et al., 2004), and it is tempting to speculate that one or more GTPases controls the membrane-binding, microtubule-binding, or NPF activities of WHAMM in a manner related to the ways that Cdc42 and Rac regulate the WASPs and WAVEs. The fact that WHAMM is positioned at the interface of actin filaments, internal membranes, and microtubules can be exploited to improve our understanding of the fundamental mechanisms by which mammalian cells control membrane dynamics in relation to multiple cytoskeletal elements.

EXPERIMENTAL PROCEDURES

Plasmids, Bacteria, Viruses, and Cells

Plasmids are listed in Table S1. For cloning, DNA fragments were amplified from cDNA templates by PCR and ligated into plasmid restriction enzyme sites. Plasmids were maintained in *E. coli* XL-1 Blue (Stratagene). Protein expression was carried out in *E. coli* BL21-Rosetta (EMD Biosciences). Bacteria were grown at 37°C. Bacmids and baculoviruses were generated using the Bac-to-Bac system (Invitrogen). Sf9 insect cells were grown in Grace's medium with 10% FBS at 28°C. Mammalian cells were grown in DMEM with 10% FBS at 37°C in 5% CO_2.

Protein Expression and Purification

Sf9 cells infected with baculoviruses encoding His-WHAMMs were lysed by freeze-thaw in His buffer (50 mM Tris, pH 8.0, 250 mM NaCl, 200 mM KCl, 5% glycerol, 0.33% NP-40, 10 μg/ml of aprotinin, leupeptin, pepstatin, and chymostatin, and 1 mM PMSF) and clarified by centrifugation at 76,000 rpm for 21 min in a TLA100.3 rotor (Beckman). Bacteria expressing His-WCA domains or GST-WHAMM truncations were lysed by sonication with 1 mg/ml lysozyme in His buffer or PBS and 200 mM KCl, respectively. His-tagged proteins were purified by Ni-NTA affinity (QIAGEN) and eluted in buffer containing 350 mM imidazole, while GST proteins were purified via glutathione affinity (GE Healthcare) and eluted in 50 mM Tris (pH 8.0) with 10 mM glutathione.

Antibodies

Anti-WHAMM WCA and CC antibodies were generated by immunizing chickens (Aves Labs) and guinea pigs (Pocono Labs) with GST-fusion proteins and affinity purified as described previously (Welch et al., 1997). The WCA antibody works robustly for immunoblotting but is not effective for immunofluorescence (IF); the CC antibody performs well for IF but weakly for blotting. Anti-GFP antibodies were generated by immunizing rabbits (Covance) with His-GFP. N-WASP antibodies were a gift from Marc Kirschner. Antibodies against Arp2/3 subunits were described previously (Welch et al., 1997). Additional antibodies recognize tubulin (U. Iowa), β-actin (Sigma), GM130, and cortactin (BD Biosciences), TGN46 (Abcam), TfnR (Santa Cruz), His5 (QIAGEN), and GAPDH (Ambion). Secondary antibodies were conjugated to HRP (Jackson Immunoresearch) for blotting and AlexaFluor 350, 488, or 568 (Invitrogen) for IF.

Cell Lysis, Fractionation, Pulldowns, Immunoblotting, and Overlays

For preparation of extracts, cells were lysed in 50 mM Tris (pH 7.6), 150 mM NaCl, 1% Triton X-100, and protease inhibitors. For fractionation, cells were lysed in 10 mM Tris (pH 7.6), 250 mM sucrose, and 1 mM EDTA by passage through a 27G needle and centrifuged at 16,000 g to remove nuclei and cellular debris. Extracts were centrifuged at 54,000 rpm in a TLA100 rotor (Beckman) for 76 min, and pellet (membrane) and supernatant (cytosol) fractions were added to equivalent volumes of SDS-PAGE sample buffer. For pulldowns of LAP-tagged proteins, Cos7 cell extracts were treated with magnetic Talon particles (Invitrogen), washed in lysis buffer, and eluted by boiling in sample buffer. For blotting, nitrocellulose membranes and tissue blots (ProSci) were probed with primary and secondary antibodies and visualized using enhanced chemiluminescence (GE Healthcare). PIP strips (Echelon Bioscience) were probed

with His-WHAMM derivatives (5 μg/ml) in PBS plus 3% BSA prior to treatment with anti-His antibodies.

Pyrene-Actin Assembly Assays

Rabbit skeletal muscle actin, pyrene-actin, and His-tagged Arp2/3 were prepared as described previously (Goley et al., 2004). His-WHAMM or His-WCA domains, purified by Ni-NTA affinity and diluted into 20 mM MOPS (pH 7.0), 100 mM KCl, 2 mM $MgCl_2$, 5 mM EGTA, 1 mM EDTA, 17 mM imidazole, and 10% glycerol were concentrated using centrifugal filter devices (Millipore). Actin (2.0 μM, 7% pyrene-labeled) was polymerized as described previously (Goley et al., 2004). Elongation rates were calculated with Microsoft Excel by measuring the slopes of pyrene curves at half of the maximal F-actin concentration.

Transfections

For expression of tagged proteins, Cos7, HeLa, or NIH 3T3 cells were transfected with 35–250 ng of DNA in 6- or 12-well plates using Lipofectamine2000 (Invitrogen). For shRNA expression, NIH 3T3 cells were transfected with empty vector or vectors encoding WHAMM shRNAs and 72 hr later retransfected with pVSV-G-mCherry. For siRNA transfections, Cos7 or HeLa cells were treated with 50 nM nonspecific or predesigned siRNAs to GAPDH, Arp3+ARPC4 (Ambion), or WHAMM (Dharmacon). Plasmid rescue was performed by cotransfecting siRNAs with 25 ng of pmCherry-WHAMM*. After 24 hr, siRNA-treated cells were transfected with 25 nM siRNA ± LAP-WHAMM plasmids (Figures 4D–4F) or pVSV-G-GFP (Figures 6D–6G). Twenty-four hours later, cells were seeded onto 12-well plates or 12 mm diameter glass coverslips and grown for another 24 hr. Cells were then collected and lysed, or processed for microscopy. For VSV-G transport assays, cells were shifted to 40.5°C for 16–24 hr before replacing culture media with media containing 10 μg/ml cycloheximide at 33°C. Cells were then incubated at 33°C for 15 or 60 min before fixation.

Cell Preparation for Fluorescence Microscopy

Drug treatments were performed using 1 μM jasplakinolide, 10 μM nocodazole, latrunculin A, or cytochalasin D (EMD Bioscience) or 10 μg/ml brefeldin A (Sigma). To detect WHAMM, cells were fixed in methanol at −20°C for 3.5 min. To visualize fluorescent fusion proteins or F-actin, cells were fixed in 2.5% paraformaldehyde for 35 min. Cells were washed with PBS and treated with primary antibodies in PBS, 1% BSA, and 1% FBS, washed, and treated with Alexa-conjugated secondary antibodies, 1 μg/ml DAPI, and/or 4 U/ml Alexa-conjugated phalloidin (Invitrogen), and mounted on glass slides using ProLong Gold anti-fade (Invitrogen). For live-cell studies, transfected cells grown on glass-bottom plates (MatTek) were transferred into DMEM, 5% FBS, 25 mM HEPES (pH 7.4), and Oxyrase to inhibit phototoxicity.

Image Acquisition and Microscopic Quantitation

All images were captured using 60× (1.40NA) or 100× (1.35NA) PlanApo objective lenses on an Olympus IX71 microscope equipped with a Photometrics Coolsnap HQ camera. For live-cell studies, images were acquired at 33°C–37°C and 10 s intervals. Images were captured in Tiff format at 16-bit resolution with Metamorph software. Using Adobe Photoshop, these data were converted to 8-bit files, and brightness/contrast levels were adjusted without altering gamma settings. Videos were compiled using ImageJ software. Microscopic quantification was done in a blinded fashion by coding coverslip samples, scoring cells that were chosen randomly, and breaking the code after visual scoring was complete. Statistical significance and p values were assessed using ANOVA and Mann-Whitney tests (Figures 4 and 5) and Student's t tests (Figure 6).

Microtubule Binding Assays

Porcine brain tubulin was precleared by centrifugation for 5 min at 2°C and 88,000 rpm in a TLA100 rotor and polymerized at 37°C in BRB80 (80 mM PIPES pH 6.8, 1 mM $MgCl_2$, and 1mM EGTA), 1 mM DTT, 1 mM GTP, and increasing amounts of taxol up to 10 μM. For sedimentation assays, WHAMM variants were overlayed onto 40% glycerol in BRB80 in the absence or presence of microtubules for 10 min prior to centrifugation for 21 min at 25°C and 40,000 rpm. Equivalent portions of supernatant and pellet fractions were resolved by SDS-PAGE.

SUPPLEMENTAL DATA

Supplemental Data include two tables, sixteen figures, and six movies and can be found with this article online at http://www.cell.com/cgi/content/full/134/1/148/DC1/.

ACKNOWLEDGMENTS

We thank members of the Welch Lab for comments on this manuscript; members of the Heald, Weis, Drubin, and Schekman Labs for technical assistance; Steve Duleh, Adrianne Pigula, and Susheela Carroll for experimental assistance; and Hans-Peter Hauri, Marc Kirschner, Craig Roy, and Roger Tsien for providing reagents. K.G.C. was supported by American Heart Association postdoctoral fellowship 0625019Y. M.D.W. was supported by NIH/NIGMS grant RO1-GM59609.

Received: November 6, 2007
Revised: March 11, 2008
Accepted: May 12, 2008
Published: July 10, 2008

REFERENCES

Appenzeller-Herzog, C., and Hauri, H.P. (2006). The ER-Golgi intermediate compartment (ERGIC): in search of its identity and function. J. Cell Sci. *119*, 2173–2183.

Benesch, S., Lommel, S., Steffen, A., Stradal, T.E., Scaplehorn, N., Way, M., Wehland, J., and Rottner, K. (2002). Phosphatidylinositol 4,5-biphosphate (PIP2)-induced vesicle movement depends on N-WASP and involves Nck, WIP, and Grb2. J. Biol. Chem. *277*, 37771–37776.

Benesch, S., Polo, S., Lai, F.P., Anderson, K.I., Stradal, T.E., Wehland, J., and Rottner, K. (2005). N-WASP deficiency impairs EGF internalization and actin assembly at clathrin-coated pits. J. Cell Sci. *118*, 3103–3115.

Cao, H., Weller, S., Orth, J.D., Chen, J., Huang, B., Chen, J.L., Stamnes, M., and McNiven, M.A. (2005). Actin and Arf1-dependent recruitment of a cortactin-dynamin complex to the Golgi regulates post-Golgi transport. Nat. Cell Biol. *7*, 483–492.

Carlier, M.F., and Pantaloni, D. (2007). Control of actin assembly dynamics in cell motility. J. Biol. Chem. *282*, 23005–23009.

Cosen-Binker, L.I., and Kapus, A. (2006). Cortactin: the gray eminence of the cytoskeleton. Physiology (Bethesda) *21*, 352–361.

Daly, R.J. (2004). Cortactin signalling and dynamic actin networks. Biochem. J. *382*, 13–25.

Eden, S., Rohatgi, R., Podtelejnikov, A.V., Mann, M., and Kirschner, M.W. (2002). Mechanism of regulation of WAVE1-induced actin nucleation by Rac1 and Nck. Nature *418*, 790–793.

Egea, G., Lazaro-Dieguez, F., and Vilella, M. (2006). Actin dynamics at the Golgi complex in mammalian cells. Curr. Opin. Cell Biol. *18*, 168–178.

Goley, E.D., and Welch, M.D. (2006). The ARP2/3 complex: an actin nucleator comes of age. Nat. Rev. Mol. Cell Biol. *7*, 713–726.

Goley, E.D., Rodenbusch, S.E., Martin, A.C., and Welch, M.D. (2004). Critical conformational changes in the Arp2/3 complex are induced by nucleotide and nucleation promoting factor. Mol. Cell *16*, 269–279.

Hehnly, H., and Stamnes, M. (2007). Regulating cytoskeleton-based vesicle motility. FEBS Lett. *581*, 2112–2118.

Hirschberg, K., Miller, C.M., Ellenberg, J., Presley, J.F., Siggia, E.D., Phair, R.D., and Lippincott-Schwartz, J. (1998). Kinetic analysis of secretory protein traffic and characterization of Golgi to plasma membrane transport intermediates in living cells. J. Cell Biol. *143*, 1485–1503.

Innocenti, M., Zucconi, A., Disanza, A., Frittoli, E., Areces, L.B., Steffen, A., Stradal, T.E., Di Fiore, P.P., Carlier, M.F., and Scita, G. (2004). Abi1 is essential for the formation and activation of a WAVE2 signalling complex. Nat. Cell Biol. *6*, 319–327.

Innocenti, M., Gerboth, S., Rottner, K., Lai, F.P., Hertzog, M., Stradal, T.E., Frittoli, E., Didry, D., Polo, S., Disanza, A., et al. (2005). Abi1 regulates the activity of N-WASP and WAVE in distinct actin-based processes. Nat. Cell Biol. *7*, 969–976.

Itoh, T., Erdmann, K.S., Roux, A., Habermann, B., Werner, H., and De Camilli, P. (2005). Dynamin and the actin cytoskeleton cooperatively regulate plasma membrane invagination by BAR and F-BAR proteins. Dev. Cell *9*, 791–804.

Kaksonen, M., Toret, C.P., and Drubin, D.G. (2006). Harnessing actin dynamics for clathrin-mediated endocytosis. Nat. Rev. Mol. Cell Biol. *7*, 404–414.

Kim, A.S., Kakalis, L.T., Abdul-Manan, N., Liu, G.A., and Rosen, M.K. (2000). Autoinhibition and activation mechanisms of the Wiskott-Aldrich syndrome protein. Nature *404*, 151–158.

Lee, M.C., Miller, E.A., Goldberg, J., Orci, L., and Schekman, R. (2004). Bi-directional protein transport between the ER and Golgi. Annu. Rev. Cell Dev. Biol. *20*, 87–123.

Legg, J.A., Bompard, G., Dawson, J., Morris, H.L., Andrew, N., Cooper, L., Johnston, S.A., Tramountanis, G., and Machesky, L.M. (2007). N-WASP involvement in dorsal ruffle formation in mouse embryonic fibroblasts. Mol. Biol. Cell *18*, 678–687.

Linardopoulou, E.V., Parghi, S.S., Friedman, C., Osborn, G.E., Parkhurst, S.M., and Trask, B.J. (2007). Human subtelomeric WASH genes encode a new subclass of the WASP family. PLoS Genet *3*, e237. 10.1371/journal.pgen.0030237.

Magdalena, J., Millard, T.H., Etienne-Manneville, S., Launay, S., Warwick, H.K., and Machesky, L.M. (2003). Involvement of the Arp2/3 complex and Scar2 in Golgi polarity in scratch wound models. Mol. Biol. Cell *14*, 670–684.

Marchand, J.B., Kaiser, D.A., Pollard, T.D., and Higgs, H.N. (2001). Interaction of WASP/Scar proteins with actin and vertebrate Arp2/3 complex. Nat. Cell Biol. *3*, 76–82.

Mattila, P.K., Pykalainen, A., Saarikangas, J., Paavilainen, V.O., Vihinen, H., Jokitalo, E., and Lappalainen, P. (2007). Missing-in-metastasis and IRSp53 deform PI(4,5)P2-rich membranes by an inverse BAR domain-like mechanism. J. Cell Biol. *176*, 953–964.

Merrifield, C.J., Perrais, D., and Zenisek, D. (2005). Coupling between clathrin-coated-pit invagination, cortactin recruitment, and membrane scission observed in live cells. Cell *121*, 593–606.

Millard, T.H., Sharp, S.J., and Machesky, L.M. (2004). Signalling to actin assembly via the WASP (Wiskott-Aldrich syndrome protein)-family proteins and the Arp2/3 complex. Biochem. J. *380*, 1–17.

Pollard, T.D. (2007). Regulation of actin filament assembly by Arp2/3 complex and formins. Annu. Rev. Biophys. Biomol. Struct. *36*, 451–477.

Pollard, T.D., and Borisy, G.G. (2003). Cellular motility driven by assembly and disassembly of actin filaments. Cell *112*, 453–465.

Prehoda, K.E., Scott, J.A., Mullins, R.D., and Lim, W.A. (2000). Integration of multiple signals through cooperative regulation of the N-WASP-Arp2/3 complex. Science *290*, 801–806.

Presley, J.F., Cole, N.B., Schroer, T.A., Hirschberg, K., Zaal, K.J., and Lippincott-Schwartz, J. (1997). ER-to-Golgi transport visualized in living cells. Nature *389*, 81–85.

Scales, S.J., Pepperkok, R., and Kreis, T.E. (1997). Visualization of ER-to-Golgi transport in living cells reveals a sequential mode of action for COPII and COPI. Cell *90*, 1137–1148.

Shikama, N., Lee, C.W., France, S., Delavaine, L., Lyon, J., Krstic-Demonacos, M., and La Thangue, N.B. (1999). A novel cofactor for p300 that regulates the p53 response. Mol. Cell *4*, 365–376.

Simpson, J.C., Nilsson, T., and Pepperkok, R. (2006). Biogenesis of tubular ER-to-Golgi transport intermediates. Mol. Biol. Cell *17*, 723–737.

Steffen, A., Rottner, K., Ehinger, J., Innocenti, M., Scita, G., Wehland, J., and Stradal, T.E. (2004). Sra-1 and Nap1 link Rac to actin assembly driving lamellipodia formation. EMBO J. *23*, 749–759.

Stradal, T.E., and Scita, G. (2006). Protein complexes regulating Arp2/3-mediated actin assembly. Curr. Opin. Cell Biol. *18*, 4–10.

Suetsugu, S., Yamazaki, D., Kurisu, S., and Takenawa, T. (2003). Differential roles of WAVE1 and WAVE2 in dorsal and peripheral ruffle formation for fibroblast cell migration. Dev. Cell *5*, 595–609.

Tsujita, K., Suetsugu, S., Sasaki, N., Furutani, M., Oikawa, T., and Takenawa, T. (2006). Coordination between the actin cytoskeleton and membrane deformation by a novel membrane tubulation domain of PCH proteins is involved in endocytosis. J. Cell Biol. *172*, 269–279.

Upadhyaya, A., and Sheetz, M.P. (2004). Tension in tubulovesicular networks of Golgi and endoplasmic reticulum membranes. Biophys. J. *86*, 2923–2928.

Welch, M.D., DePace, A.H., Verma, S., Iwamatsu, A., and Mitchison, T.J. (1997). The human Arp2/3 complex is composed of evolutionarily conserved subunits and is localized to cellular regions of dynamic actin filament assembly. J. Cell Biol. *138*, 375–384.

Yamazaki, D., Suetsugu, S., Miki, H., Kataoka, Y., Nishikawa, S., Fujiwara, T., Yoshida, N., and Takenawa, T. (2003). WAVE2 is required for directed cell migration and cardiovascular development. Nature *424*, 452–456.

Yan, C., Martinez-Quiles, N., Eden, S., Shibata, T., Takeshima, F., Shinkura, R., Fujiwara, Y., Bronson, R., Snapper, S.B., Kirschner, M.W., et al. (2003). WAVE2 deficiency reveals distinct roles in embryogenesis and Rac-mediated actin-based motility. EMBO J. *22*, 3602–3612.

Yarar, D., Waterman-Storer, C.M., and Schmid, S.L. (2005). A dynamic actin cytoskeleton functions at multiple stages of clathrin-mediated endocytosis. Mol. Biol. Cell *16*, 964–975.